

# Salicylaldehyde Phenylhydrazone: A New Highly Selective Fluorescent Lead (II) Probe

Diganta Kumar Das · Priyanka Goswami · Smita Sarma

Received: 22 September 2012 / Accepted: 31 January 2013 / Published online: 14 February 2013  
© Springer Science+Business Media New York 2013

**Abstract** The fluorescence intensity of salicylaldehyde phenylhydrazone (**L**), in 1:1 (v/v) CH<sub>3</sub>OH:H<sub>2</sub>O was enhanced by *ca.* 100 times with a blue shift in emission maximum, on interaction with Pb<sup>2+</sup> ion. No enhancement in fluorescent intensity of **L** was observed on interaction with metal ions - Na<sup>+</sup>, K<sup>+</sup>, Ca<sup>2+</sup>, Cu<sup>2+</sup>, Ni<sup>2+</sup>, Zn<sup>2+</sup>, Cd<sup>2+</sup> and Hg<sup>2+</sup>. This signal transduction was found to occur via photoinduced electron transfer (PET) mechanism. A 1:1 complexation between Pb<sup>2+</sup> and **L** with log β=7.86 has been proved from fluorescent and UV/Visible spectroscopic data. The detection limit of Pb<sup>2+</sup> was calculated to be 6.3 × 10<sup>-7</sup> M.

**Keywords** Lead · Fluorescence · Probe · Salicylaldehyde phenylhydrazone · Photoinduced electron transfer

## Introduction

The design and synthesis of fluorescent probes for transition and heavy metal ions is currently of prime importance for both environmental and biological applications [1, 2]. While transition metal ions play an important role in many fundamental physiological processes in organisms, heavy metal ions can often have a profoundly detrimental effect upon them. Among heavy metal ions, lead is the most abundant and occupies the second position among the list of toxic metals and is often encountered for contaminating the environment due to its wider distribution in nature [3]. As one of the major pollutants of the environment, Pb<sup>2+</sup> toxicity is an ongoing danger to the human health and environment particularly in children [4, 5]. Lead (II) ions affect almost every organ and system of the human body, mainly the nervous

system. Lead toxicity causes various symptoms such as anaemia, muscle paralysis, loss of memory, disorder of blood and even mental retardation [6–8]. Lead also increases blood pressure level and causes weakness in fingers, wrists and ankles. Moreover high exposures to lead can result in severe damage of kidneys and brain [9, 10]. Lead toxicity is mainly triggered by various sources such as air, drinking water, soil etc. Thus, the development of effective fluorescent probes [11, 12] for distinguishing lead ions from alkali, alkaline earth metal and transition metal ions [13–15] is quite important for detecting the presence of lead (II) in contaminated sources [16] as well as in the human body.

The importance of fluorescent probes has increased considerably over the past decade due to their easy use in solutions and owing to their high sensitivity and selectivity for trace analytes [17] and real time detection [18]. Thus, in the past decade, considerable efforts have been made to develop Pb<sup>2+</sup>-responsive fluorescent probes due to their sensitivity, simplicity and adaptability to different platforms that facilitate routine screening [19]. As most of the heavy metals are known fluorescence quenchers, the development of selective as well as sensitive probes based on fluorescent enhancement for Pb<sup>2+</sup> presents a challenge.

While a good number of fluorescent probes have been developed for Zn<sup>2+</sup> [20, 21] and other heavy metal ions such as Cd<sup>2+</sup> [22, 23], Hg<sup>2+</sup> [24–27] etc., very few have been reported for Pb<sup>2+</sup>. A ratiometric and selective fluorescent probe for Pb<sup>2+</sup> based on polypeptide scaffolds equipped with a microenvironment-sensitive fluorophore has been reported [28]. Lu et al. utilized catalytic DNAs as a unique class of biosensors for Pb<sup>2+</sup> [29]. A turn-on ratiometric fluorescent probe for Pb<sup>2+</sup> was described by Cao and coworkers [30]. Ma et al. also reported a fluorescent probe based on the Pb<sup>2+</sup>-catalyzed hydrolysis of phosphodiester [31]. A new fluorescent probe for Pb<sup>2+</sup> based on a triazolothiadiazin derivative immobilized in polyvinyl chloride membrane was also developed [32]. A pyrene-containing

D. K. Das (✉) · P. Goswami · S. Sarma  
Department of Chemistry, Gauhati University,  
Guwahati 781 014 Assam, India  
e-mail: digkdas@yahoo.com

fluorescent probe with high selectivity for  $\text{Pb}^{2+}$  was also reported [33]. Yoon and coworkers reported a highly selective fluorescent probe for  $\text{Pb}^{2+}$  [34]. An imidazole-annelated ferrocene derivative was synthesized [35] which was found to be a highly sensitive multichannel chemical probe for  $\text{Pb}^{2+}$ .

Herein, we report a fluorescent probe derived from the condensation of salicylaldehyde and phenylhydrazine which showed fluorescent peak at  $\lambda_{\text{max}}$  value 529 nm on excitation by 410 nm photon. A fluorescent enhancement (accompanied by a blue shift) of *ca.* 100 times was registered by  $\text{Pb}^{2+}$  in 1:1 (v/v)  $\text{CH}_3\text{OH}:\text{H}_2\text{O}$  while other metal ions -  $\text{Na}^+$ ,  $\text{K}^+$ ,  $\text{Ca}^{2+}$ ,  $\text{Cu}^{2+}$ ,  $\text{Ni}^{2+}$ ,  $\text{Zn}^{2+}$ ,  $\text{Cd}^{2+}$  and  $\text{Hg}^{2+}$  had no effect on the fluorescent property of the probe. The binding ratio, binding constant and detection limits were also determined.

## Experimental

### Materials and Methods

Phenylhydrazine was purchased from Loba Chemie while salicylaldehyde was obtained from Merck. All the metal salts (sulphate) and methanol were purchased from Merck. All chemicals were of analytical grade and used without further purification. The metal salts were recrystallised from water (Millipore). Metal salt solutions ( $10^{-6}\text{M}$ ) were prepared in 0.1 M phosphate buffer solution (PBS), pH7.0. Fluorescence spectra measurements were performed in a HITACHI FL-2500 fluorescence spectrophotometer using a quartz cuvette and both the excitation and emission band passes were set at 10.0 nm. A 4.0  $\mu\text{M}$  solution of **L** in 1:1 (v/v)  $\text{CH}_3\text{OH}:\text{H}_2\text{O}$  (PBS, pH7.0) was used in all the experiments.

UV/Visible spectra were recorded in a Shimadzu UV 1800 spectrophotometer.  $^1\text{H}$  NMR and  $^{13}\text{C}$  NMR spectra were recorded in a Bruker Ultrashield 300 spectrometer. All NMR spectra were recorded in  $\text{CDCl}_3$  at room temperature and the chemical shift values are reported in  $\delta$  values (ppm) relative to TMS.

Electrochemical measurements were carried out in a CHI 600B Electrochemical Analyzer (USA), which consisted of a three-electrode cell arrangement. The electrode environment consisted of a platinum disc as the working electrode,  $\text{Ag}-\text{AgCl}$  (3 M  $\text{NaCl}$ ) as the reference electrode and  $\text{NaNO}_3$  (0.1 M) as the supporting electrolyte. The working electrode was cleaned by polishing with 0.1  $\mu\text{m}$  alumina slurry using a polishing kit (CHI), followed by sonication in distilled water for 5 min.

Synthesis of the ligand **L** was carried out according to the reported procedure [36] as follows; 0.105 mL (*ca.* 0.1 mol) salicylaldehyde was dissolved in 10 mL ethanol and an ethanolic solution of 0.100 mL (*ca.* 0.1 mol) phenylhydrazine

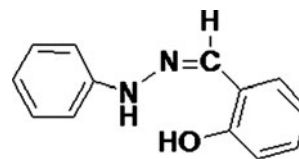
was added. The resulting mixture was stirred in a magnetic stirrer for 30 min. The brownish yellow solid thus obtained was filtered, washed with distilled water and allowed to dry for carrying out the further experiments.

**FTIR (KBr):** 3290.56  $\text{cm}^{-1}$  ( $\nu_{\text{C}=\text{N}}$ ), 3051.39  $\text{cm}^{-1}$  ( $\nu_{\text{C}-\text{H}}$ ), 1269.16  $\text{cm}^{-1}$ , 3421.72  $\text{cm}^{-1}$  ( $\nu_{\text{O}-\text{H}}$ ), 1,570 and 1600.42  $\text{cm}^{-1}$  ( $\nu_{\text{C}-\text{N}}$ ) and 1482.75  $\text{cm}^{-1}$  ( $\nu_{\text{C}=\text{C}}$ ).  
 **$^1\text{H}$ NMR** ( $\text{CDCl}_3$ ,  $\delta$  ppm, TMS): 10.88(s,1H), 7.87 (s,1H), 7.5 (s,1H), 7.31–7.24 (m,3H), 7.14–6.91 (m,6H), 4.8 (s,1H) (Scheme 1).

## Results and Discussion

The metal ion sensing property of **L** ( $10^{-6}\text{M}$ ) towards  $\text{Na}^+$ ,  $\text{K}^+$ ,  $\text{Ca}^{2+}$ ,  $\text{Cu}^{2+}$ ,  $\text{Ni}^{2+}$ ,  $\text{Zn}^{2+}$ ,  $\text{Cd}^{2+}$ ,  $\text{Pb}^{2+}$  and  $\text{Hg}^{2+}$  has been investigated by fluorescence spectroscopy. Fluorescence of **L** in 1:1 (v:v)  $\text{CH}_3\text{OH}:\text{H}_2\text{O}$  was examined employing different excitation wavelengths from 250 nm to 410 nm at an interval of 10 nm in absence of any metal ions or in presence of any one of the above metal ions. The concentration ratio between **L** and the metal ion was kept at 1:1. No significant change in fluorescent property of **L** was observed when no metal ion was present. Fluorescence of **L** was found to enhance sharply by *ca.* 100 times when  $\text{Pb}^{2+}$  ion was present in the solution and the excitation wavelength was 410 nm.

Figure 1 shows the fluorescence response of **L** at zero and different added concentration of  $\text{Pb}^{2+}$  ion (from 0.49  $\mu\text{M}$  to 4.3  $\mu\text{M}$ ). The fluorescence titration studies of **L** with  $\text{Pb}^{2+}$  revealed that the intensity of the fluorescent peak at 529 nm increased gradually with the increasing concentration of  $\text{Pb}^{2+}$  ion. The increase in the fluorescence intensity on addition of  $\text{Pb}^{2+}$  ion at the final added concentration was calculated to be *ca.* 100 times to the original one. Moreover, a blue shift in the  $\lambda_{\text{max}}$  value was also observed from 529 nm to 504 nm. Inset of Fig. 1 depicts the plot of  $I/I_0$  as a function of  $\text{Pb}^{2+}$  ion concentration, where  $I$  is the intensity at a given concentration of  $\text{Pb}^{2+}$  ion (at  $\lambda_{\text{max}}$  value 504 nm) and  $I_0$  is the intensity at zero concentration of  $\text{Pb}^{2+}$  ion (at  $\lambda_{\text{max}}$  value 529 nm). The  $I/I_0$  value was found to increase linearly ( $R^2=0.9942$ ) up to the value of *ca.* 100 till the final concentration of  $\text{Pb}^{2+}$  became 4.3  $\mu\text{M}$  and remained constant thereafter. The concentration ratio of **L** and  $\text{Pb}^{2+}$  ion at saturated fluorescent intensity being *ca.* 1:1.



**Scheme 1** Structure of **L**

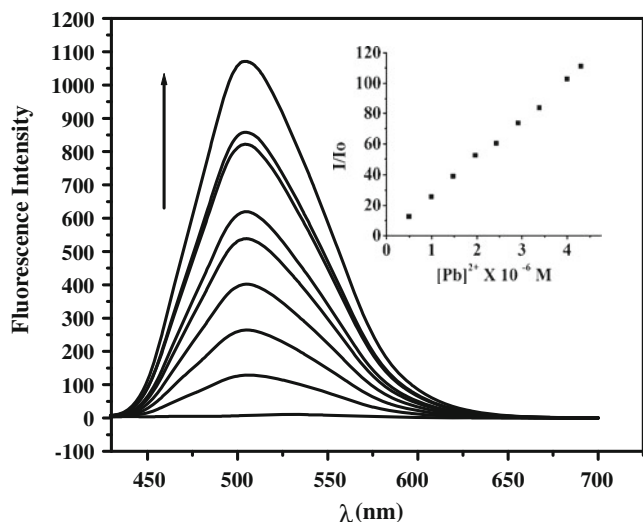


**Fig. 1** Fluorescence emission spectra of **L** when 0, 0.49, 0.99, 1.47, 1.96, 2.43, 2.91, 3.38, 3.84 and  $4.3 \times 10^{-6}$  M  $\text{Pb}^{2+}$  ion was present in 1:1(v/v)  $\text{CH}_3\text{OH}:\text{H}_2\text{O}$ . ( $\lambda_{\text{ex}}=410$  nm;  $\lambda_{\text{emi}}=450 - 600$  nm; Inset: plot of  $I/I_0$  as a function of  $\text{Pb}^{2+}$  ion concentration)

The detection limit of **L** for  $\text{Pb}^{2+}$  was calculated to be  $6.3 \times 10^{-7}$  M.

Similar fluorescence titrations were also performed with the other metal ions  $\text{Na}^+$ ,  $\text{K}^+$ ,  $\text{Ca}^{2+}$ ,  $\text{Cu}^{2+}$ ,  $\text{Ni}^{2+}$ ,  $\text{Zn}^{2+}$  and  $\text{Cd}^{2+}$  using 410 nm as the excitation wavelength. The results showed that titration with these metal ions did not induce any significant changes in the fluorescence emission spectra of **L**. Addition of  $\text{Zn}^{2+}$ ,  $\text{Ca}^{2+}$  and  $\text{Hg}^{2+}$  ions caused a slight increase of about 3 times in the fluorescence spectra of **L**. However, addition of all the other metal ions triggered a very small quenching effect in the fluorescence intensity of **L**. The metal ion selectivity profile of **L** is depicted in Fig. 2 by a bar diagram to show the effect of diverse metal ions, at  $4.3 \times 10^{-6}$  M concentration, on the fluorescent intensity of **L**. The diagram clearly portrays the sensitivity and selectivity of the probe towards  $\text{Pb}^{2+}$  ions.

The number of  $\text{Pb}^{2+}$  ions bound to **L** and the binding constant was determined by plotting  $\log[(I_0 - I)/(I - I_{\text{max}})]$

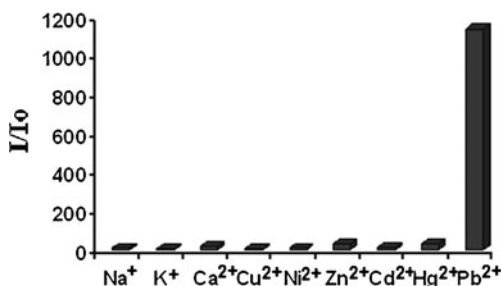


**Fig. 2** Bar diagram showing effect of 1 equivalent of different metal ions ( $4.3 \times 10^{-6}$  M) on the fluorescent intensity of **L**, in 1:1(v/v)  $\text{CH}_3\text{OH}:\text{H}_2\text{O}$

against  $\log [\text{Pb}^{2+}]$  (Fig. 3) [37], the slope and the X-axis intercept representing the number of  $\text{Pb}^{2+}$  ions bound and the log of binding constant ( $\beta$ ) respectively. A least squares fitting of data ( $R^2=0.9864$ ) yielded the slope to be 1.082, indicating the binding of one  $\text{Pb}^{2+}$  ion to **L** and the log  $\beta$  value was calculated as 7.86.

The UV/visible spectra of **L**, recorded in 1:1(v/v)  $\text{CH}_3\text{OH}:\text{H}_2\text{O}$  showed two absorption peaks with  $\lambda_{\text{max}}$  values at 300 nm and 346 nm. Figure 4 displays the changes in the absorption spectra of **L** on increasing the concentration of  $\text{Pb}^{2+}$  ions (0.49  $\mu\text{M}$  to 4.3  $\mu\text{M}$ ) in the solution. While no changes in the absorption spectra were recorded on addition of the other metal ions to **L**, it was revealed that titration with  $\text{Pb}^{2+}$  ions resulted in a remarkable change. Addition of  $\text{Pb}^{2+}$  ions resulted in an increase in the absorbance of the peak at 300 nm and a decrease in the absorbance of the peak at 346 nm. Inception of a new absorption peak was observed at 650 nm with the addition of  $\text{Pb}^{2+}$  ion. This new absorption peak should be responsible for the high fluorescence of **L**:  $\text{Pb}^{2+}$  adduct excited by 410 nm photon. In order to further confirm the number of  $\text{Pb}^{2+}$  ions bound to **L** and the binding constant,  $\log [(A_0 - A_s)/(A_s - A_{\text{max}})]$  value was plotted against  $\log[\text{Pb}^{2+}]$  from the absorption titration studies (Fig. 4). Here,  $A_0$ ,  $A_s$  and  $A_{\text{max}}$  are the absorbances of **L** at zero, at an intermediate and at saturated concentration of  $\text{Pb}^{2+}$  ion respectively. A least square fitting of the data ( $R^2=0.9976$ ) yielded the slope as 1.006 confirming 1:1 binding between **L** and  $\text{Pb}^{2+}$ . The binding constant log  $\beta$  was calculated to be 7.45 which is close to the value calculated from the fluorescence data.

We also tested whether interaction between **L** and  $\text{Pb}^{2+}$  was effected by other metal ions such as  $\text{Na}^+$ ,  $\text{K}^+$ ,  $\text{Ca}^{2+}$ ,  $\text{Cu}^{2+}$ ,  $\text{Ni}^{2+}$ ,  $\text{Zn}^{2+}$ ,  $\text{Cd}^{2+}$  and  $\text{Hg}^{2+}$  or not. For this purpose 1  $\mu\text{M}$  solution of **L** already having 10  $\mu\text{M}$   $\text{Pb}^{2+}$  ion was prepared and fluorescence intensity recorded. A particular metal ion was added so that its concentration becomes

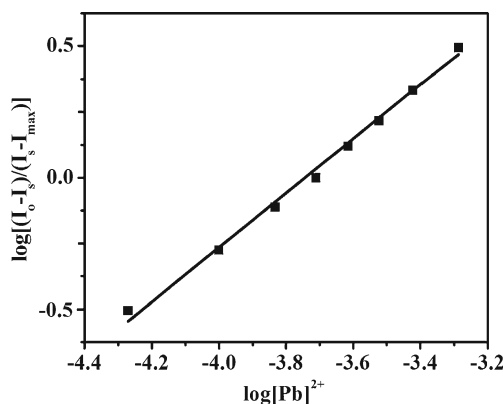


**Fig. 3** Plot of  $\log[(I_0 - I_s)/(I_s - I_{\text{max}})]$  versus  $\log[\text{Pb}^{2+}]$  for titration of **L** against  $\text{Pb}^{2+}$  in 1:1(v/v)  $\text{CH}_3\text{OH}:\text{H}_2\text{O}$ . The plot shows a slope of 1.082 ( $R^2=0.9864$ ) indicating binding of one  $\text{Pb}^{2+}$  ion to **L** with log  $\beta=7.86$

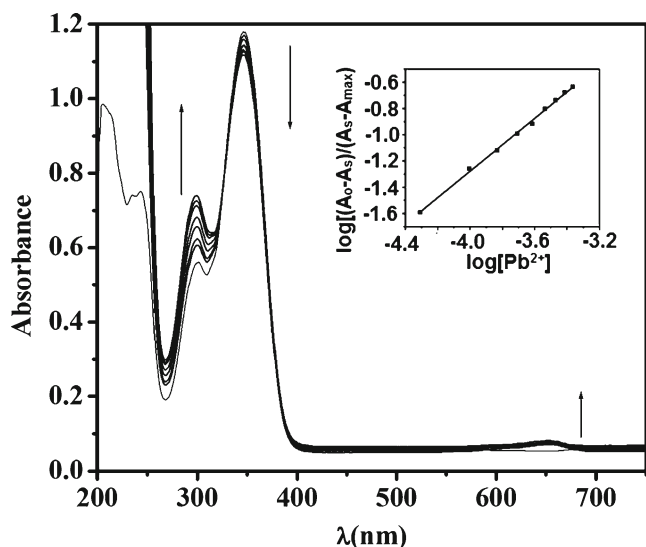


**Fig. 4** Change in the UV/visible spectra of **L** when the concentration of  $\text{Pb}^{2+}$  ion was varied from 0 to  $4.3 \times 10^{-6}$  M. Inset: Plot of  $\log [(A_o - A_s)/(A_s - A_\infty)]$  as a function of  $\text{Pb}^{2+}$  ion concentration. The plot shows a slope of 1.006 ( $R^2 = 0.9976$ ) indicating binding of one  $\text{Pb}^{2+}$  ion to **L** with  $\log \beta = 7.45$

10  $\mu\text{M}$  and fluorescence intensity recorded. It was found that the fluorescence intensity of **L**+ $\text{Pb}^{2+}$  ion system was effected only to a very small extent by other metal ions. The result has been summarised by a bar diagram of fluorescence intensity ratio of **L**+ $\text{Pb}^{2+}$  ion to **L**+ $\text{Pb}^{2+}$  in presence of other metal ions (Fig. 5). This confirms that binding between **L** and  $\text{Pb}^{2+}$  ion is much stronger than the interaction between **L** and other metal ions.

The remarkable change in the fluorescent signal transduction of **L** on interaction with  $\text{Pb}^{2+}$  may be explained on the basis of the disruption of efficient photoinduced electron transfer (PET) mechanism prevailing in **L** [38]. In **L**, the PET process occurs due to the transfer of electron density, originating at the lone pairs of electrons on N atoms of the phenylhydrazine group to the LUMO of the fluorophore part (salicylaldehyde). This results in quenching of the fluorescence intensity of **L**. Both from the fluorescence and

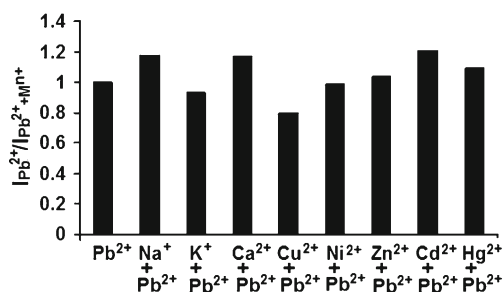


**Fig. 5** Fluorescent response of **L** (1  $\mu\text{M}$ ) containing 10  $\mu\text{M}$   $\text{Pb}^{2+}$  to the selected 10  $\mu\text{M}$  metal ions  $\text{M}^{n+}$  ( $\text{Na}^+$ ,  $\text{K}^+$ ,  $\text{Ca}^{2+}$ ,  $\text{Cu}^{2+}$ ,  $\text{Ni}^+$ ,  $\text{Zn}^{2+}$ ,  $\text{Cd}^{2+}$  and  $\text{Hg}^{2+}$ ) in 1:1(v/v)  $\text{CH}_3\text{OH}:\text{H}_2\text{O}$ . The excitation wavelength,  $\lambda_{\text{ex}}$  was set at 410 nm

UV/Visible spectral titrations, it is evident that one  $\text{Pb}^{2+}$  ion binds to **L**, likely through the two N-atoms present in the phenylhydrazine moiety. Thus interaction of  $\text{Pb}^{2+}$  ion with **L** disrupts the PET process and results the enhancement in fluorescence intensity.

In PET process, the driving force ( $\Delta G_{\text{et}}$ ) from the receptor group to the excited fluorophore is expressed by the modified Weller [39] equation as follows,  $\Delta G_{\text{et}} = -E_s - E_{\text{red.fluor}} + E_{\text{ox.receptor}}$ , where  $E_s$ ,  $E_{\text{red.fluor}}$  and  $E_{\text{ox.receptor}}$  denote the singlet energy, reduction potential of the fluorophore and the oxidation potential of the receptor respectively. The cyclic voltammetric response of **L** ( $10^{-5}$  M) in 1:1(v/v)  $\text{CH}_3\text{OH}:\text{H}_2\text{O}$  was investigated by utilizing a platinum disc as the working electrode and  $\text{Ag}/\text{AgCl}$  as the reference electrode. A reversible redox couple was obtained which displayed the reduction peak potential value at  $-0.020$  V and the oxidation peak at  $+0.3365$  V. However, in the presence of different concentration of  $\text{Pb}^{2+}$  ion (0.49  $\mu\text{M}$  to 4.3  $\mu\text{M}$ ), it was observed that at the final added concentration, the reduction peak value shifted to  $-0.176$  V and the oxidation peak shifted to  $+0.044$  V towards the negative direction (Fig. 6). Thus, from the modified Weller equation, it is evident that the binding of  $\text{Pb}^{2+}$  ion to **L** increases the  $\Delta G_{\text{et}}$  value, consequently leading to the cessation of the PET process. No change in the cyclic voltammogram of **L** was observed when metal ions -  $\text{Na}^+$ ,  $\text{K}^+$ ,  $\text{Ca}^{2+}$ ,  $\text{Cu}^{2+}$ ,  $\text{Ni}^{2+}$ ,  $\text{Zn}^{2+}$ ,  $\text{Cd}^{2+}$  and  $\text{Hg}^{2+}$  were added into the electrolytic medium alone or together. From this electrochemical data, the selective interaction between **L** and  $\text{Pb}^{2+}$  could be further confirmed.

The selectivity of **L** for  $\text{Pb}^{2+}$  over  $\text{Na}^+$ ,  $\text{K}^+$ ,  $\text{Ca}^{2+}$ ,  $\text{Cu}^{2+}$ ,  $\text{Ni}^{2+}$ ,  $\text{Zn}^{2+}$ ,  $\text{Cd}^{2+}$  and  $\text{Hg}^{2+}$  is particularly important because  $\text{Pb}^{2+}$  targets both  $\text{Ca}^{2+}$ - and  $\text{Zn}^{2+}$ -binding sites in vivo [40, 41] and  $\text{Cd}^{2+}$ ,  $\text{Hg}^{2+}$  and  $\text{Cu}^{2+}$  are metal ions that frequently interfere with  $\text{Pb}^{2+}$  ion detection. To summarize, we have presented an efficient yet simple probe derived from the condensation of

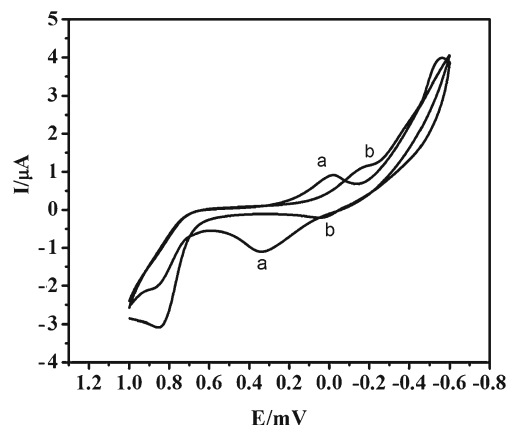


**Fig. 6** Cyclic voltammetric response of (a) 1  $\mu\text{M}$  solution of **L** in 1:1(v/v)  $\text{CH}_3\text{OH}:\text{H}_2\text{O}$ ; and (b) 1  $\mu\text{M}$  solution of **L** in presence of 4.3  $\mu\text{M}$   $\text{Pb}^{2+}$  in 1:1 (v/v)  $\text{CH}_3\text{OH}:\text{H}_2\text{O}$



phenylhydrazine and salicylaldehyde, which displayed a high selectivity for  $\text{Pb}^{2+}$  ion in 1:1 (v:v)  $\text{CH}_3\text{OH}:\text{H}_2\text{O}$  at excitation wavelength 410 nm. This excitation wavelength is much higher than the UV/Visible absorption peaks of the probe. The interaction between the probe and  $\text{Pb}^{2+}$  ion results the high fluorescence intensity. The presence of the other metal ions in the solution does not offer any hindrance to the enhancement in the fluorescence intensity. The remarkable increase in the fluorescence intensity of *ca* 100 times on interaction with  $\text{Pb}^{2+}$  was accompanied by a blue shift in the emission spectra. A 1:1 complexation between **L** and  $\text{Pb}^{2+}$  ion is proved to be formed which snaps the PET process in **L** leading to fluorescent enhancement.

**Acknowledgment** UGC, New Delhi and DST, New Delhi are thanked for financial support to the Department. PG thanks the former for fellowship under RFSMS.

## References

- Valeur B, Leray I (2000) Design principles of fluorescent molecular sensors for cation recognition. *Coord Chem Rev* 205:3–40
- Prodi L, Bolletta L, Montalti M, Zaccheroni N (2000) Luminescent chemosensors for transition metal ions. *Coord Chem Rev* 205:59–83
- Yoosaf K, Ipe BI, Suresh CH, Thomas KG (2007) In situ synthesis of metal nanoparticles and selective naked-eye detection of lead ions from aqueous media. *J Phys Chem C* 111:12839–12847
- Ragan P, Turner T (2009) Working to prevent lead poisoning in children: getting the lead out. *J Am Acad Phys Asst* 22:40–45
- Needleman HL (1992) Human lead exposure. CRC Press, Boca Raton
- Florin TA, Brent TMW, Weitzman M (2005) The need for vigilance: the persistence of lead poisoning in children. *Pediatrics* 115:1767–1768
- Garza A, Vega R, Soto E (2006) Cellular mechanisms of lead neurotoxicity. *Med Sci Monit* 12:RA57–RA65
- Magyar JS, Weng TC, Stern CM, Dye DF, Rous BW, Payne JC, Bridgewater BM, Mijovilovich A, Parkin G, Zaleski JM, Penner-Hahn JE, Godwin HA (2005) Reexamination of lead (II) coordination preferences in sulfur-rich sites: implications for a critical mechanism of lead poisoning. *J Am Chem Soc* 127:9495–9505
- Abbate C, Buceti R, Munao F, Giorgianni C, Ferreri G (1995) Neurotoxicity induced by lead levels: an electrophysiological study. *Int Arch Occup Environ Health* 66:389–392
- Manahan SE (1994) Environmental chemistry. CRC Press, Boca Raton
- Basabe-Desmouts L, Reinhoudt DN, Crego-Calama M (2007) Design of fluorescent materials for chemical sensing. *Chem Soc Rev* 36:993–1017
- Valeur B, Leray I (2007) Ion-responsive supramolecular fluorescent systems based on multichromophoric calixarenes: a review. *Inorg Chim Acta* 360:765–774
- Jiang P, Guo Z (2004) Fluorescent detection of zinc in biological systems: recent development on the design of chemosensors and biosensors. *Coord Chem Rev* 248:205–229
- Prodi L (2005) Luminescent chemosensors: from molecules to nanoparticles. *New J Chem* 29:20–31
- Valeur B, Leray I (2000) Design principles of fluorescent molecular sensors for cation recognition. *Coord Chem Rev* 205:3–40
- Métivier R, Leray I, Valeur B (2003) A highly sensitive and selective fluorescent molecular sensor for Pb (II) based on a calix [4] arene bearing four dansyl groups. *Chem Commun* 8:996–997
- de Silva AP, Fox DB, Huxley AJM, Moody TS (2000) Combining luminescence, coordination and electron transfer for signalling purposes. *Coord Chem Rev* 205:41–57
- Zhang J, Campbell RE, Ting AY, Tisen RY (2002) Creating new fluorescent probes for cell biology. *Nat Rev Mol Cell Biol* 3:906–918
- Yao J, Li J, Owens J, Zhong W (2011) Combining DNAzyme with single-walled carbon nanotubes for detection of Pb(II) in water. *Analyst* 136:764–768
- Goswami P, Das DK (2012) N, N, N, N-tetradentate macrocyclic ligand based selective fluorescent sensor for zinc (II). *J Fluorescence* 22:1081–1085
- Gong Z-L, Zhao B-X, Liu W-Y, Lv H-S (2011) A new highly selective “turn-on” fluorescent sensor for zinc ion based on a pyrazoline derivative. *J Photochem Photobiol A* 218:6–10
- Goswami P, Baruah S, Das DK (2010) 2,7-dichlorofluorescein, a fluorescent sensor to detect  $\text{Cd}^{2+}$  over  $\text{Na}^+$ ,  $\text{K}^+$ ,  $\text{Ca}^{2+}$ ,  $\text{Cu}^{2+}$ ,  $\text{Ni}^{2+}$  and  $\text{Zn}^{2+}$ . *Indian J Chem A* 49:1617–1620
- Goswami P, Das DK (2012) A new highly sensitive and selective fluorescent cadmium sensor. *J Fluorescence* 22:391–395
- Jiang J, Liu W, Cheng J, Yang L, Jiang H, Bai D, Liu W (2012) A sensitive colorimetric and ratiometric fluorescent probe for mercury species in aqueous solution and living cells. *Chem Comm* 48:8371–8373
- Yan F, Cao D, Wang M, Yang N, Yu Q, Dai L, Chen L (2012) A new rhodamine-based “off-on” fluorescent chemosensor for Hg(II) ion and its application in imaging Hg(II) in living cells. *J Fluorescence* 22:1249–1256
- Fan J, Peng X, Wang S, Liu X, Li H, Sun S (2012) A fluorescence turn-on sensor for  $\text{Hg}^{2+}$  with a simple receptor available in sulphide-rich environments. *J Fluorescence* 22:941–955
- Liu J, Yu M, Wang X-C, Zhang Z (2012) A highly selective colorimetric sensor for  $\text{Hg}^{2+}$  based on nitrophenyl-aminothiourea. *Spectrochim Acta Part A* 93:245–249
- Deo S, Godwin HA (2000) A selective, ratiometric fluorescent sensor for  $\text{Pb}^{2+}$ . *J Am Chem Soc* 122:174–175
- Liu J, Yi L (2003) A colorimetric lead biosensor using DNAzyme-directed assembly of gold nanoparticles. *J Am Chem Soc* 125:6642–6643
- Hou C, Xiong Y, Fu N, Jacquot CC, Squier TC, Cao H (2011) Turn-on ratiometric fluorescent sensor for  $\text{Pb}^{2+}$  detection. *Tetrahedron Lett* 52:2692–2696
- Sun M, Shangguan D, Ma H, Nie L, Li X, Xiong S, Liu G, Thiemann W (2003) Simple Pb II fluorescent probe based on PbII-catalyzed hydrolysis of phosphodiester. *Biopolymers* 72:413–420
- Aksuner N (2011) Development of a new fluorescent sensor based on a triazolo-thiadiazin derivative immobilized in polyvinyl chloride membrane for sensitive detection of lead(II) ions. *Sensors Actuators B* 157:162–168
- Ma L, Li H, Wu Y (2009) A pyrene-containing fluorescent sensor with high selectivity for lead (II) ion in water with dual illustration of ground-state dimer. *Sensors Actuators B* 143:25–29
- Kwon JY, Jang YJ, Lee YJ, Kim KM, Seo MS, Nam W, Yoon J (2005) A highly selective fluorescent chemosensor for  $\text{Pb}^{2+}$ . *J Am Chem Soc* 127:10107–10111
- Zapata F, Caballero A, Espinosa A, Tárraga A, Molina P (2009) Imidazole-annulated ferrocene derivatives as highly selective and sensitive multichannel chemical probes for Pb(II) cations. *J Org Chem* 74:4787–4796

36. Love BE, Jones EG (1999) The use of salicylaldehyde phenylhydrazine as an indicator for the titration of organometallic reagents. *J Org Chem* 64:3755–3756
37. Dong X, Yang Y, Sun J, Liu Z, Bi-F L (2009) Two-photon excited fluorescent probes for calcium based on internal charge transfer. *Chem Commun* 26:3883–3885
38. Ashokkumar P, Ramakrishnan VT, Ramamurthy P (2011) Photo-induced Electron Transfer (PET) based  $Zn^{2+}$  fluorescent probe: transformation of turn-on sensors into ratiometric ones with dual emission in acetonitrile. *J Phys Chem A* 2011:14292–14299
39. Bryan AJ, de Silva AP, Rupasinghe RADD, Sodayake KRAS (1989) Photo-induced electron transfer as a general design logic for fluorescent molecular sensors for cations. *Biosensors* 4:169–179
40. Goldstein GW (1993) Evidence that lead acts as a calcium substitute in second messenger metabolism. *Neurotoxicology* 14:97–102
41. Kulatilleke CP, Silva SA, Eliav Y (2006) A coumarin based fluorescent photoinduced electron transfer cation sensor. *Polyhedron* 25:2593–2596